

Implementation Penalties for Nonlinear Interference Estimation with Linear Least Squares Longitudinal Power Monitoring

Original

Implementation Penalties for Nonlinear Interference Estimation with Linear Least Squares Longitudinal Power Monitoring / Andrenacci, Lorenzo; Nespola, Antonino; Straullu, Stefano; Jiang, Yanchao; Piciaccia, Stefano; Bosco, Gabriella; Pileri, Dario. - ELETTRONICO. - (In corso di stampa), pp. 1-3. (Intervento presentato al convegno Optical Fiber Communication Conference (OFC) tenutosi a San Francisco (USA) nel 30 March - 03 April 2025).

Availability:

This version is available at: 11583/2996581 since: 2025-01-14T12:02:56Z

Publisher:

Optica Publishing Group

Published

DOI:

Terms of use:

This article is made available under terms and conditions as specified in the corresponding bibliographic description in the repository

Publisher copyright

(Article begins on next page)

Implementation Penalties for Nonlinear Interference Estimation with Linear Least Squares Longitudinal Power Monitoring

Lorenzo Andrenacci,^{1,*} Antonino Nespola,² Stefano Straullu,² Yanchao Jiang,¹
Stefano Piciaccia,³ Gabriella Bosco,¹ and Dario Pileri¹

¹ DET, Politecnico di Torino, C.so Duca degli Abruzzi 24, 10129 Torino, Italy

² LINKS Foundation, Via Pier Carlo Boggio 61, 10138 Torino, Italy

³ Cisco Photonics Italy S.r.l., Via S. M. Molgora 48/C, 20871 Vimercate (MB), Italy

*lorenzo.andrenacci@polito.it

Abstract: We investigate the practical implementation penalty of using hard-decided symbols to generate the reference signal in linear least squares longitudinal power monitoring for nonlinear interference estimation, both numerically and over a 17x65-km experimental setup. © 2025 The Author(s)

1. Introduction

Linear least-squares (LLS) longitudinal power monitoring (LPM) is an algorithm that estimates the power evolution of the channel of interest (COI) in a WDM comb, using only information available at the receiver DSP [1]. The estimated power profile can then be applied to a variety of network performance monitoring and optimization tasks [2], such as anomaly detection [1] and semi-automatic line-system provisioning [3]. As an example, LPM has been proposed as a potential solution for segregating the received noise into amplified spontaneous emission (ASE) and nonlinear interference (NLI) [2,4]. In fact, noise segregation is an active research topic [5], as it enables a simple and straightforward estimation of the optimal launch power of the COI.

To compute the power profile, LLS LPM requires limited information from the receiver DSP [1], with the key inputs being the received (noisy) constellation symbols and the corresponding noise-free transmit symbols. However, in a real-time receiver, obtaining the noise-free transmit symbols is not trivial. In [6], using a different LPM algorithm (correlation-based), the authors showed that the transmit sequence can be replaced by a simple hard-decision (HD) of the received constellation. They found that this substitution introduces only a simple offset in the estimated power profile, which can be easily compensated for.

In this work, we aim to analyze the practical effects of this power offset on NLI estimation in the context of noise segregation, resorting to LLS-based LPM. A preliminary analysis is conducted over a simple simulation scenario and its results are validated in an experimental transmission over a 17×65 -km SSMF link.

2. Principle and limitations

The NLI estimation algorithm discussed in this work was proposed in [4] and resorts to LLS-based LPM [1]. It consists in estimating the power profile evolution $\gamma' = \frac{8}{9}\gamma\mathbf{P}$ of a WDM optical signal \mathbf{A} in the propagation direction and using it to reconstruct its first-order nonlinear approximation term \mathbf{A}_1 . This term carries information on NLI and can be expressed in matrix form as $\mathbf{A}_1 \simeq \mathbf{G}\gamma'$, where \mathbf{G} is a perturbation matrix computed from a reference version of the transmitted signal \mathbf{A}_{ref} [1]. The nonlinear SNR can then be computed as:

$$\text{SNR}_{\text{NL}} = \frac{1}{\zeta} \frac{G_{\mathbf{A}_{\text{ref}}}}{G_{\mathbf{A}_1}} \quad (1)$$

where $G_{\mathbf{A}_{\text{ref}}}$ and $G_{\mathbf{A}_1}$ are the power spectral densities (PSDs) of \mathbf{A}_{ref} and \mathbf{A}_1 , here assumed flat over the channel bandwidth. The factor ζ , instead, is a correction term introduced to account for the cross-channel interference (XCI) contribution to NLI, since LPM includes only self-channel interference (SCI). As proposed in [4], $\zeta = N_{\text{ch}}^{1/4}$, where N_{ch} is the number of WDM channels. However, \mathbf{A}_{ref} is reconstructed based on the transmitted symbol sequence. This sequence can either be known, as in the case of pilot symbols, or retrieved after FEC decoding. In the first case, the pilot sequence cannot be too long to avoid a reduction in spectral efficiency, while in the second case retrieving the original transmitted sequence is not trivial, due to the presence of large interleavers. A practical solution is to perform a simple HD on the received constellation, with the trade-off that some errors are introduced

in the reconstructed sequence. The effect of these errors on the power profile estimations (PPEs) is an offset, which was first observed in [6] for the correlation-based LPM. However, a power offset in the PPEs potentially degrades the performance of the NLI estimation algorithm, since Kerr-induced NLI is a power-dependent effect.

3. Numerical investigation

We first investigate numerically the performance penalty arising from using HD symbols for LLS-based LPM. To this purpose, we resort to the simple setup shown in Fig. 1(a). The transmitted WDM signal consists of $N_{\text{ch}} = 11$ 150-GHz spaced DP-16QAM channels, modulated at $R_s = 128$ Gbaud and shaped by an SRRC filter with roll-off 0.1. The per-channel power is set to $P_{\text{ch}} = 5$ dBm. The COI is the central one. The link is composed by 4×50 -km identical SMF spans, with attenuation $\alpha_{\text{dB}} = 0.2$ dB/km, CD coefficient $\beta_2 = -21.28$ ps²/km and nonlinearity coefficient $\gamma = 1.3$ 1/W/km. Each span is followed by a noiseless EDFA which compensates for the previous span loss. Fiber propagation is modeled according to the split-step Fourier method (SSFM). Before entering the receiver, noise loading is performed on the propagated signal. In order to test a wide range of BER values, the OSNR was spanned between 10 dB and 30 dB, with step 1 dB. Then, the received signal enters the RX DSP and undergoes CD compensation, adaptive equalization, CPR and decoding. The output of CPR is extracted and used to perform LPM, with 2^{20} input samples and a spatial granularity set to $\Delta z = 1$ km. A few examples of results using the HD sequence for LPM are displayed in Fig. 1(b). The PPE is consistent with the theoretical curve when there are no errors in the HD sequence. However, as the OSNR decreases (and BER increases), an estimation offset appears, degrading the quality of the PPE. This offset is reported in Fig. 1(c) for all tested BER values. It was computed as the difference in power at the beginning of the third span (i.e., $z = 100$ km) between the PPE computed with an error-free sequence and that computed with the HD sequence (which will be referred to as HD-PPE). A fitting has been performed to find a simple relation between the offset and the BER. This relation can be expressed as a scaling factor, i.e., ψ [dB] = $k \cdot \text{BER}$ with $k \simeq 100$ for the considered scenario and BER in linear units. This simple formula can be used to correct the HD-PPEs and improve the quality of the NLI estimation.

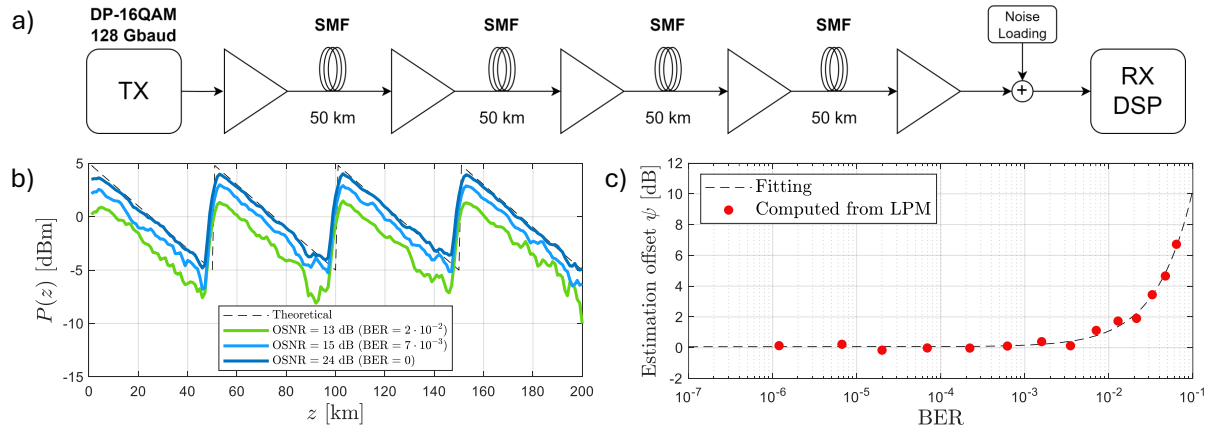


Fig. 1. a) Simulation setup. b) Power profiles computed starting from HD sequences for varying OSNR (and BER) values. c) Estimation offset for varying BER values.

4. Experimental setup and results

We then experimentally test the NLI estimation algorithm and the effect of the HD-PPEs in a more realistic and challenging scenario, reported in Fig. 2(a). In fact, as can be observed from Fig. 1(c), the estimation offset starts becoming significant for $\text{BER} > 10^{-3}$, which is also the range that defines the maximum reach of the employed modulation format in practical cases. In the experiment, we transmit a DP-16QAM 64-Gbaud WDM signal consisting of $N_{\text{ch}} = 30$ channels, shaped by an SRRC filter with roll-off 0.1 and spaced by $\Delta f = 100$ GHz. The per-channel power P_{ch} is varied between -1 dBm and 5 dBm with step 2 dB. The COI is channel 15, centered at 193.2 THz and transmitted with a commercial coherent transceiver. The interfering channels, instead, are generated with a WaveShaper (WS) placed after an ASE. source. The signal is propagated through an optical link consisting of 17×65 -km SSMF spans. An in-line EDFA (ILA), working in automatic gain control mode and compensating for the previous span loss, terminates each span. At the receiver side, the COI is filtered by a tunable optical filter (TOF) centered at the COI center frequency and attenuated by a VOA to adjust its power before entering the commercial transceiver. It is then sampled at 96 GSa/s by the transceiver's analog-to-digital converter (ADC) and the acquired samples are downloaded for offline processing. After front-end corrections and resampling at a rate of 2 sample-per-symbol, the signal samples enter the coherent DSP, where CDC, frequency offset compensation

(FOC), LMS-based 2×2 MIMO fractionally-spaced equalization and BPS CPR are performed. The output of the CPR stage is then fed to the LPM algorithm. The number of samples used as input is 2^{17} and the spatial resolution is set to $\Delta z = 2$ km. 100 data acquisitions are performed for each tested power value. The average BER for all cases is reported in Fig. 2(b). It shows that the optimal power is included in the tested values, being around $P_{\text{ch}} \sim +1$ dBm. The NLI is estimated according to (1). In order to assess the effect of HD, SNR_{NL} is evaluated in three ways: with PPEs computed with error-free sequences, with HD-PPEs without BER-based offset correction, and with HD-PPEs with offset correction. As a reference, we also compute the theoretical SNR_{NL} with the aid of the closed-form model (CFM) [7]. The results are displayed in Fig. 2(c). When using an error-free reference sequence, the algorithm yields relatively accurate results, with a mean absolute error with respect to the CFM equal to 0.5 dB. However, when resorting to HD and BER is high, the estimation strongly degrades, yielding a mean absolute error of 3.5 dB. The results can be improved if, before using (1), the offset in HD-PPEs is corrected, based on the BER. In this case, the estimation highly improves and the mean absolute error decreases to 0.8 dB. The additional error is due to the fact that only the offset is corrected, but the PPEs are still affected by the noise in the reference sequence.

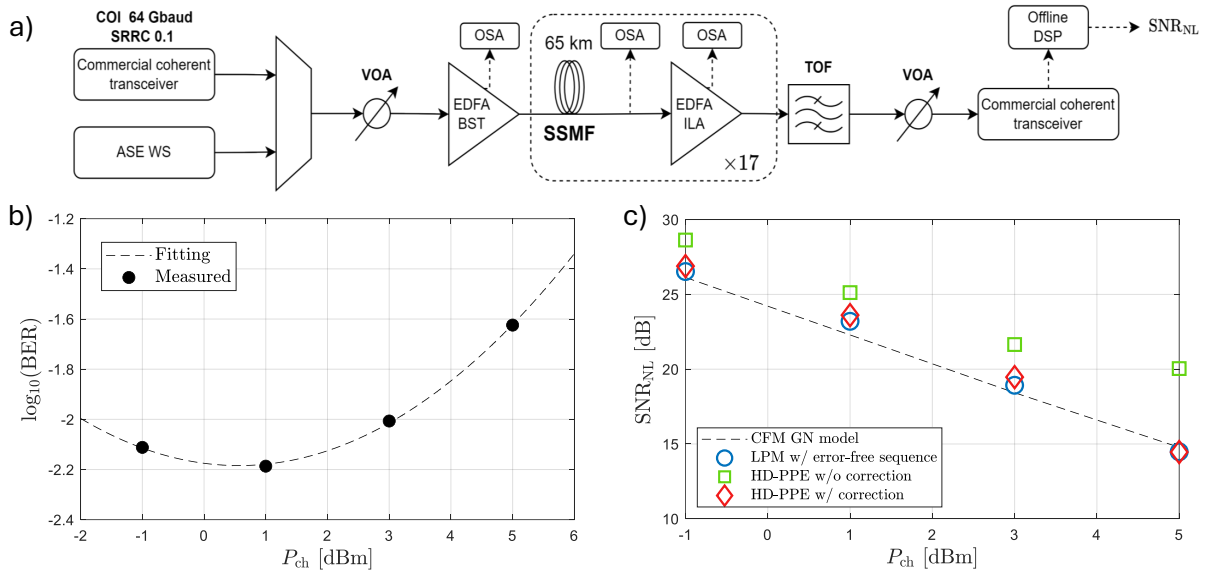


Fig. 2. a) Experimental setup. EDFA BST: Booster EDFA. OSA: optical spectrum analyzer. VOA: Variable Optical Attenuator. b) BER curve for each tested power value. c) Nonlinear SNR computed with CFM, PPE with error-free sequence, HD-PPE with and without offset correction for each tested power value.

5. Conclusions

In this work, we presented practical considerations on the implementation penalties for NLI estimation based on LLS-based LPM. We first numerically investigated the estimation offset introduced when using HD reference sequences in place of error-free sequences (e.g., pilots or post-FEC) in the LPM algorithm. Our results show that – in logarithmic units – the power offset in HD-PPEs is related to the pre-FEC BER through a simple scaling factor. We then performed NLI estimation in a more challenging experimental setup consisting of 17×65 -km SSMF spans. We found that, after applying a BER-based correction to HD-PPEs, the NLI estimation algorithm accuracy degraded by only 0.3 dB.

References

1. T. Sasai et al., “Linear Least Squares Estimation of Fiber-Longitudinal...,” JLT 42 (6), 1955–1965, 2024.
2. M. R. Sena et al., “Link Tomography: A Tool for Monitoring Optical Network...,” proc. ECOC 2024, p. M3E.5.
3. H. Nishizawa et al., “Semi-automatic line-system provisioning with an integrated...,” JOCN 16 (2), 894–904, 2024.
4. L. Andrenacci et al., “Nonlinear Noise Estimation using Linear Least Squares-based...,” proc. ECOC 2024, p. M3E.4.
5. I. Andrenacci et al., “Machine-learning-based technique to establish ASE or Kerr...,” JOCN 16 (4), 481–492, 2024.
6. J. Chang et al., “Demonstration of longitudinal power profile estimation using commercial transceivers...,” proc. ECOC 2023, p. Tu.A.2.2.
7. P. Poggiolini et al., “Closed Form Expressions of the Nonlinear Interference for UWB Systems,” proc. ECOC 2022, p. Tu1D.1.